Geochemistry and petrology of two kimberlites at Krishtipadu from Gooty cluster, Andhra Pradesh, southern India – evidence of kimberlite magmatism and a possible carbonatite association within Palaeoproterozoic lower Cuddapah basin

P. Ramesh Chandra Phani[1],
Prabir Sengupta[2], *Sudeshna Basu*[3]

[1]Cyient Limited, Hyderabad, India

[2]Bedrock Mineral Resource Consulting, Dubai, UAE

[3]Cairn India Oil & Gas, Vedanta Limited, Gurugram, India

Abstract. This paper addresses geochemical and petrological aspects of two outcropping kimberlites (5023 and 5119) of the Gooty cluster, emplaced in carbonate sediments of Vempalli Formation of lower Cuddapah basin at Krishtipadu, Anantapur district, Andhra Pradesh, southern India. These pipes were discovered by the Rio Tinto Exploration Group in the recent past. The 5023 kimberlite is enriched in olivine and serpentine while the 5119 pipe possesses haematitised olivine pseudomorphs. The field, textural characteristics and whole rock geochemistry qualify both the pipes for hypabyssal kimberlite breccias of Group-I type similar to world's classical occurrences. The carbon and oxygen stable isotope data, aided with field and petrological studies, indicates existence of possible carbonatite (sovite) phase associated with the 5119 kimberlite.

The two kimberlites appear to be originated from a low degree of partial melting ranging from 0.5 to 2.5%. Enrichment of LREE with a high LREE/HREE ratio indicates fractionation at the mantle source region. Whole rock geochemistry supports their diamondiferous nature. Presence of crustal xenoliths post-dates subsequent emplacement of the two pipes to lower Cuddapah sedimentation (2.4 Ga), manifesting kimberlite magmatism. These pipes are the only known Group-I kimberlites from the Proterozoic Cuddapah Basin and therefore warrant detailed investigations.

Introduction

Extensive exploration for kimberlite pipes carried out by multinational companies in the last decade with the implementation of latest field methods and laboratory analytical techniques has led to the discovery of many new diamondiferous kimberlite pipes in the eastern Dharwar craton (EDC) of southern India. These kimberlite discoveries include both outcropping and concealed pipes which are authentically proved to possess better grades than those discovered by various organisations

in the past. Some of these new discoveries are characteristically unique in their field geological, lithological, mineralogical and petrological behaviours.

The EDC has been proved to be fertile for emplacement of kimberlites [Chalapathi Rao et al., 2016] and recorded more than 150 kimberlite pipes in Wajrakarur kimberlite field (WKF), Narayanpet kimberlite field (NKF), Raichur kimberlite field (RKF) and Tungabhadra kimberlite field (TKF). The diamond-rich WKF, evidencing more than 45 kimberlite occurrences, has an areal extent of over 9500 km^2 [Chatterjee et al., 2008; Das Sharma and Ramesh, 2013; Phani and Raju, 2017; Shaikh et al., 2016; Smith et al., 2013]. The WKF is further subdivided into clusters of kimberlite pipes viz., Wajrakarur, Lattavaram, Chigicherla, Kalyanadurgam, Anumpalli and Timmasamudram. In addition, the crescent shaped Cuddapah basin on the eastern side of WKF, has recorded more than 47 lamproite occurrences in the northern margin and central part, distributed in five lamproite fields [Ravi et al., 2018 and references therein] (Figure 1a).

In addition to the above occurrences, CRA Exploration (India) Pvt. Ltd. (CRAEI Ltd., a member of the Rio Tinto Group) during its reconnaissance operations in parts of Andhra Pradesh state in early 2000s,
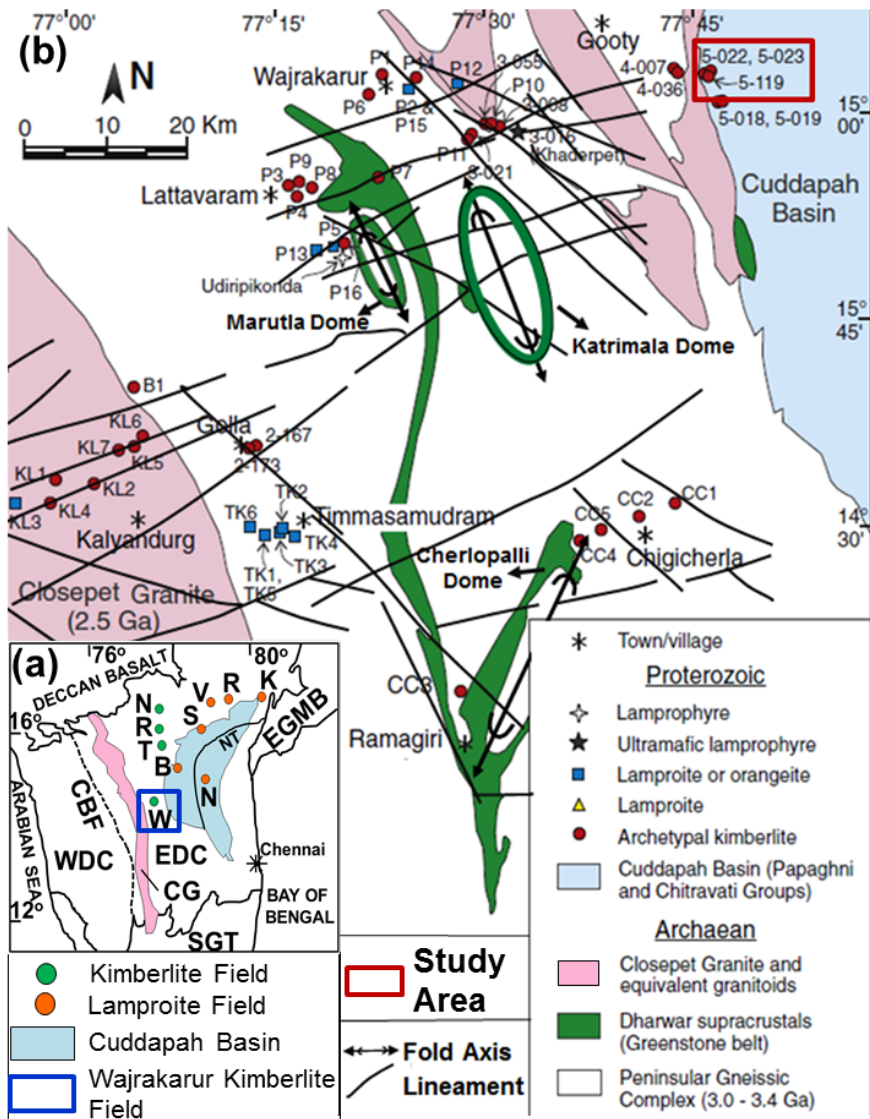
(b)

N

0   10   20 Km

77°'00'   77°'15'   77°'30'   77°'45'

Gooty

Wajrakarur

P1 P14 P12 3-055
P6 P2 & P10
P15 3-008
P11 3-016 (Khaderpet)
3-021

4-007
4-036

5-022, 5-023
← 5-119
5-018, 5-019

15°'00'

Cuddapah Basin

P3 P9 P8
Lattavaram P4 P7
P5
P13
Udiripikonda P16

Marutla Dome

Katrimala Dome

15°'45'

B1

KL6
KL7 KL5 Golla 2-167
KL1 KL2 2-173
KL4 TK2
KL3 TK6 Timmasamudram
Kalyandurg TK4
TK1, TK3
TK5

CC2 CC1
CC5
CC4 Chigicherla

14°'30'

Closepet Granite (2.5 Ga)

Cherlopalli Dome

(a)

76°   80°

DECCAN BASALT

N V R K
R S
N T
R B
T

EGMB

CBF NT N

ARABIAN SEA

WDC EDC Chennai

CG BAY OF BENGAL

SGT

CC3

Ramagiri

● Kimberlite Field
● Lamproite Field
▨ Cuddapah Basin
☐ Wajrakarur Kimberlite Field

☐ **Study Area**

↔ **Fold Axis**
Lineament

∗   Town/village
Proterozoic
✧   Lamprophyre
★   Ultramafic lamprophyre
■   Lamproite or orangeite
▲   Lamproite
●   Archetypal kimberlite
▨   Cuddapah Basin (Papaghni and Chitravati Groups)
Archaean
▨   Closepet Granite and equivalent granitoids
▨   Dharwar supracrustals (Greenstone belt)
☐   Peninsular Gneissic Complex (3.0 - 3.4 Ga)

Figure 1. (a) Regional geological map of Dharwar craton. (b) Location and simplified geological map of the Wajrakarur Kimberlite Field showing 5023 and 5119 kimberlites of Gooty cluster in (Modified after [*Shaikh et al.,* 2016]). Lineaments after [*Phani,* 2015]. Kimberlite Field (KF): N – Narayanpet, R – Raichur, T – Tungabhadra, W – Wajrakarur, Lamproite Field (LF): B – Banaganapalli, K – Krishna, N – Nallamalai, R – Ramadugu, S – Somasila, V – Vattikodu. CG – Closepet Granite, CBF – Chitradurga Boundary Fault, EDC – Eastern Dharwar Craton, EGMB – Eastern Ghat Mobile Belt, NT – Nallamalai Thrust, SGT – Southern Granulite Terrain, WDC – Western Dharwar Craton.

has discovered a new cluster of kimberlites situated at a distance of 25 km due SE of Gooty (Gutti), a small town in Anantapur district. This new cluster, christened as Gooty Kimberlite Cluster (GKC) by the Rio Tinto, comprises eight pipes viz., 4-007, 4-036, 5-022, 5-023, 5-119, 5-018, 5-019 and 5-028 [*CRAEI,* 2004; *Radhakrishna,* 2007] sprawling in the Archaean PGC country as well as lower Cuddapah sedimentaries at the westernmost convex margin of the Cuddapah basin. While five kimberlite pipes of the GKC are covered under siliciclastic colluvium within granite gneiss country, three outcropping pipes (5022, 5023 and 5119) peep through the Palaeoproterozoic lower Cuddapah sedimentary horizons viz., Vempalli Forma-

tions occurring at Krishtipadu village (77°46′48.28″ E, 15°3′50.78″ N; 1:250K toposheet #57E). There were apprehensions among some workers whether or not the GKC pipes are actually emplaced in Proterozoic Cuddapah sedimentaries [*Chalapathi Rao,* 2012]. Evidenced from extensive field traverses, we hereby confirm that three pipes of the GKC i.e., 5022, 5023 and 5119, are undoubtedly emplaced in lower Cuddapahs comprising dolomites, chert, shale and mudstones (see Table 1 in [*Phani et al.,* 2020]). Their occurrence within a background of rocks of Vempalli Formation and the presence of clasts of similar rock types confirm their emplacement in lower Cuddapahs. The geological contact of Vempalli dolomites and Archaean granitoids is situated at about 1 km towards west of these intrusions. Thus these intrusions act as finger prints of kimberlite magmatism in the lower Cuddapah sedimentaries and these are the only known kimberlites so far within the Cuddapah basin sediments whilst the Chelima and Zamgarajupalli occurrences are lamproites (Figure 1b). The discovery of GKC pipes by CRAEI has indeed reduced the wide gap hitherto existing between the WKF on the western side and Nallamalai lamproites in the middle part of Cuddapah basin. The present investigation preludes petrography, geochemistry and petroge-

nesis of two outcropping kimberlite occurrences (5023 and 5119) of the GKC.

Field Geological Aspects

Field traverses have been conducted during December, 2017 − January, 2018. The outcrops (5023 and 5119) have been accessed by the authors using toposheet, geological map, hand-held GPS, information present in reconnaissance permit (RP) report available from Indian Bureau of Mines website along with the guidance from local villagers.

The geological domain, in which the two GKC pipes of present study are emplaced, is situated close to the contact zone of Archaean granitoids and Palaeoproterozoic sedimentary rocks of Cuddapah basin. The extensively investigated Cuddapah basin extends approximately for an area of 44,500 km^2 and lies unconformably on Archaean granite-greenstone basement of the Dharwar craton; the basin is popular for offering understanding about not only regional tectono-stratigraphic evolution of Precambrian crust of India but also configuration of super continent assembly and associated magmatism [Kale, 2016; Nagaraja Rao et al., 1987]. The two kimberlites are intruded in the lower

Cuddapah carbonate rocks of Vempalli Formation of Papaghni Group of the Papaghni sub-basin (PSB, see Table 2 in [*Phani et al.,* 2020]). The PSB typically represents an intracratonic basinal sequence dating back to the Palaeoproterozoic in Indian sub-continent. During field traverses, it was observed that the upper part of the dolomite formation consists of red scaly shales with thin silty sandy laminae indicating a shore face-inner-shelf deposition, possibly during the maximum rise of sea level in the first cycle of sedimentation [*Saha and Tripathy,* 2012]. The two kimberlite outcrops are exposed on the hill slope portion (Δ350 m MSL) amidst a mixed terrain of pediplain and pediment of PSB dominated by dolomitic limestones. The dolomite/dolomitic limestones are associated red shale and chert veins, striking in NNE-SSW trend with a dip of $12°$ towards SE and exhibit common karst geomorphic features. Intense brecciation is observed at the contact of kimberlite intrusion and dolomite wherein drucy crystalline calcite occurs as massive outcrop and also as veins. An EW trending reverse fault runs across the Archaean-Proterozoic contact along which these kimberlites are presumably emplaced.

The 5023 pipe is exposed in khaki green colour, dominated by dolomite xenoliths that exhibit similar

Figure 2. Field photographs. 5023 pipe: (a) Outcrop boulders. (b) Kimberlite with angular dolomite clasts. (c) A large hexagon shaped dolomite xenolith. 5119 pipe: (d) Outcrop of kimberlite breccia. (e) Kimberlite insitu boulder. (f) Carbonatite-Kimberlite breccia showing ferruginised olivine macrocrysts. Note shale, dolomite xenoliths. Scale bar length 11 cm.

textural and physical characteristics to the surrounding country rock (*Vempalli dolomites*) (Figure 2a). As per the observations made in field, the kimberlitic portion is present up to 70–80% with well-developed olivine macrocrysts (0.2–0.5 cm) ranging from rounded to sub-rounded. The rock shows serpentinisation and contains large angular crustal xenoliths (0.5 to 20 cm; 30–40% by volume) giving rise to brecciated appearance (Figure 2b and Figure 2c). Several gains of ilmenites (0.2–0.3 mm) are seen in the surface gravels around. A GPS based outcrop mapping suggests a surface extent of 115 × 70 m (0.8 Ha) ovoid shaped body. The 5023 pipe possesses a small eruption pulse (0.01 Ha) on the eastern periphery as evidenced by a small detached outcrop.

The 5119 pipe crops out as a brecciated greyish brown shade rock occurring in the valley portion (Figure 2d). This kimberlite appears to be associated with buff white crystalline calcite, presumably representing a carbonatite phase. The kimberlitic material exhibits inequigranular texture with highly haematitised olivine macrocrysts ranging from 1 mm to 4 mm. The percentage of kimberlitic material associated with crystalline calcite varies (10–90% by volume) within the outcrop (Figure 2e). Numerous crystalline calcite veins also cut

across the brecciated rock. The calcite shows texture which may be a primary product of quenching similar to Benfontein kimberlite sill of South Africa and carbonatite lavas of Oldoinyo Lengai of Tanzania [*Dawson,* 1980; *Dawson et al.,* 1987]. At the contact of pipe with host, intense brecciation with crystalline calcite matrix and with increased dolomite clasts of varied sizes (0.3 to 15 cm) is observed (Figure 2f). A GPS based mapping indicated an outcrop surface area of 70×21 m (~ 0.15 Ha).

Sampling and Analytical Methods

All the field traverses, sampling and analyses were carried out afresh for this study. In total, fourteen freshest possible rock samples (1.5 to 2 kg) were carefully collected from the outcrops. Six samples from 5023 kimberlite and eight samples from 5119 with varied proportion of carbonatite and kimberlite material (90% carbonatite + 10% kimberlite and 90% kimberlite + 10% carbonatite) were collected. Each sample was divided into two parts, one for petrography and the other for whole rock geochemistry. Polished thin-sections were made at Gita Laboratory, Kolkata. For geochemical analysis, the samples were gently broken and crustal

xenoliths were hand-picked and discarded. The major, trace and rare earth elements were determined using standard sample preparation process, dissolution and analytical techniques at an NABL (National Accreditation Board for Testing and Calibration Laboratories) accredited laboratory at Bangalore, India, well-versed with geochemical analysis of kimberlites and related rocks. For QA-QC purpose, repetitive analyses were conducted and several certified reference materials were used for calibration. The crystalline calcite portion was carefully separated by gentle crushing and manual picking and six samples were analysed for carbon and oxygen stable isotopes at the Wadia Institute of Himalayan Geology, Dehradun by adopting precise and standard procedures.

Petrography

Both the kimberlites show inequigranular and brecciated texture under the microscope. The common mineral assemblage includes olivine, serpentine and magnetite as microcrysts and picroilmenite as microphenocryst within an indiscernible matrix of similar mineralogy along with shale and dolomite as crustal xenoliths. The 5119 pipe shows primary crystalline calcite appearing to be

magmatic. The detailed petrography of each pipe is described in the following paragraphs.

The 5023 kimberlite contains essentially a combination of two generation olivines i.e., the early-formed macrocrysts and late-formed microphenocrysts of olivine in a non-micaceous matrix. The matrix comprises a suite of altered spinels and perovskite mineral phases. The kimberlitic matrix essentially contains fine-grained calcite lacking palimpsest textures along with lesser proportion of fine-grained serpentine. The presence of angular xenolithic fragments of different types of crustal rocks gives the kimberlite an appearance of polymictic breccia (Figure 3a). The olivine macrocrysts often appear bleached due to intense alteration or calcification. Numerous phlogopite phenocrysts are distributed all through the groundmass and also as clusters. The oxides in the matrix are either fine shells with hematite atolls to magnetite/Cr-spinel cores, or they are coarse aggregates of these minerals plus perovskite and subordinate fresh ilmenite. The olivine macrocrysts appear to have undergone furruginisation and are invariably found to be haematitised (Figure 3b). The dolomite clasts are intensely serpentinised as evidenced by several veins cutting across. At places the clasts are also furruginised (Figure 3c). There are also iso-
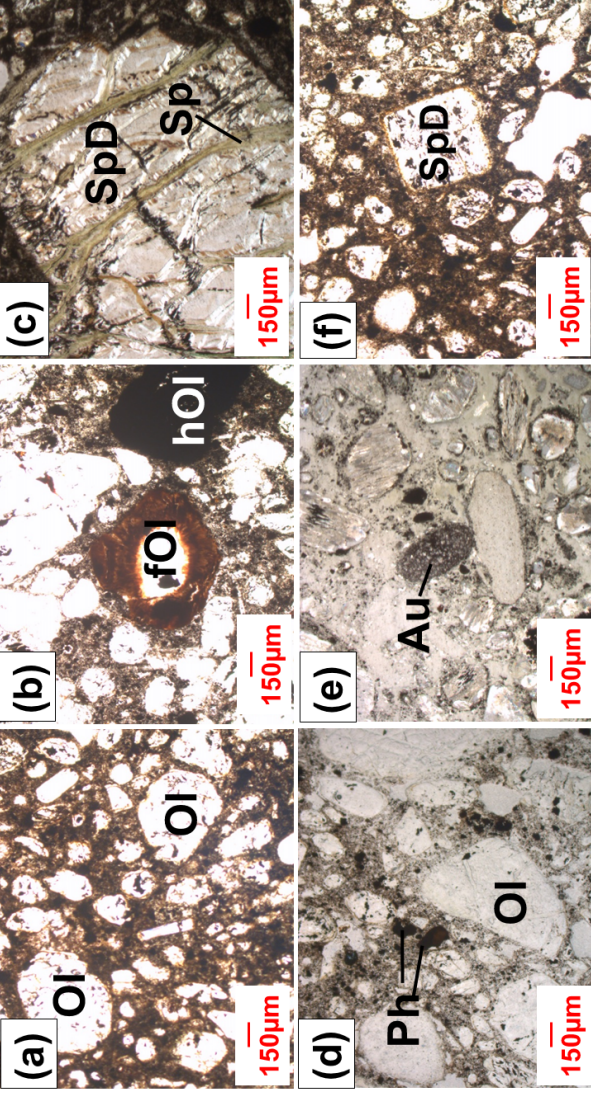
Figure 3. Photomicrographs of 5023 pipe. (a) Altered olivine macrocrysts within a fine-grained groundmass. (b) Olivine macrocrysts under furruginisation and haematitised olivine macrocyst and dolomite xenolith. (c) Heavily serpentinised dolomite (spD) intervened by serpentine (Sp). (d) Heavily altered olivine macrocrysts with phenocrysts of phlogopite. (e) An autholith of kimberlite amidst heavily altered olivine pseudomorphs. (f) Square shaped serpentinised dolomite xenolith within an inequigranular kimberlite matrix. Abbreviations: Au – kimberlite autolith, fOl – furruginised olivine, hOl – haematitised olivine, Ol – Olivine, Ph – phlogopite, SpD – serpentinised dolomite.

lated single perovskites usually under 0.1 mm. Secondary magnetite is often prominent in vein or networks in the serpentinised olivines (Figure 3d and Figure 3e). The dolomite xenoliths are often intensely serpentinised. The kimberlite contains several picroilmenites, to 0.5 mm size, which can be single crystals or clusters which tend to have a perovskite margin. The matrix is obscured by a heavy impregnation of hematite/goethite (Figure 3f). The overall mineral assemblages, inequigranular texture and the presence of crustal xenoliths qualifies the 5023 to be a matrix supported hypabyssal kimberlite breccia of Group-I variety.

The 5119 kimberlite predominantly comprises subhedral to anhedral olivine macrocrysts within a fine-grained groundmass of serpentine, phlogopite, perovskite, calcite which is imperceptible. The olivine macrocrysts are encircled by calcite reaction rim (Figure 4a). The crustal xenoliths include smudgy ferruginous shale which is found at the top horizon in Vempalli Formations (Figure 4b). The calcite grains display high-order interference colours, perfect rhombohedral cleavage, twinkling and twinning under crossed-polars. A sharp contact between kimberlite and crystalline calcite is clearly noticed (Figure 4c). The crystalline calcite portion of the 5119 kimberlite displays typical magmatic crystalline
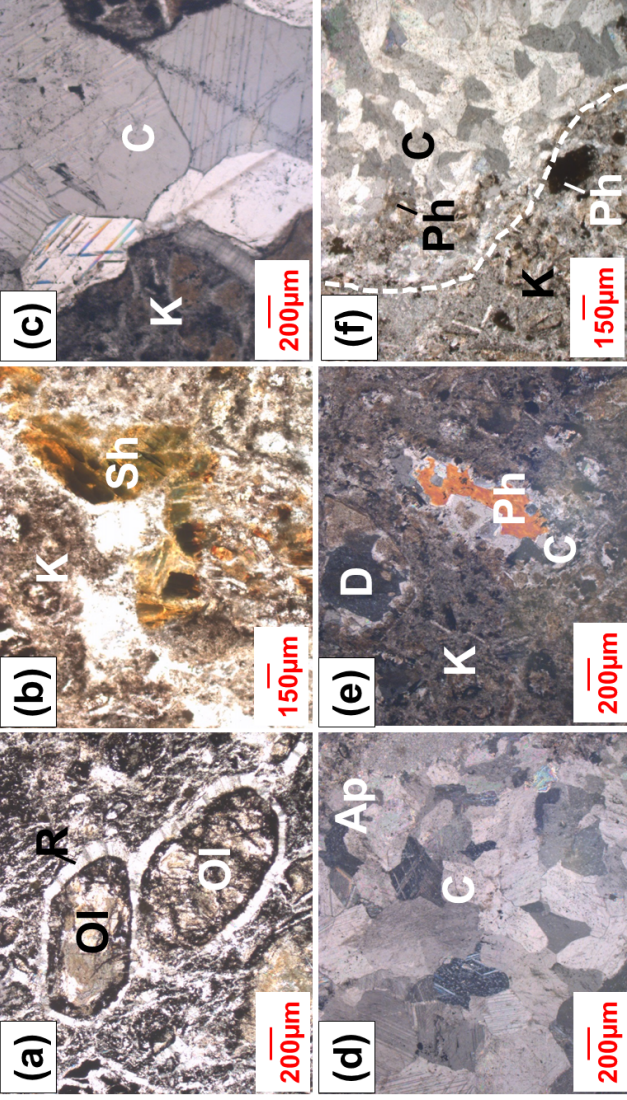
Figure 4. Photomicrographs of 5119: (a) and (b) Olivine macrocrysts displaying reaction rims. (c) A xenolith of shale. (Sh) within kimberlite matrix. (c) Sharp contact of kimberlite and carbonatite. Note calcite vein intruding to kimberlite. (a) Magmatic crystalline texture of carbonatite. (b) Poikilitic growth of phlogopite phenocrysts associated with carbonatite phase. (d) Dolomite xenoliths with calcified peripheries. Macrocrystic olivine pseudomorphs with calcite reaction rims. Abbreviations: C – carbonatite, D – dolomite, K – kimberlite, Ol – olivine, Ph – phlogopite, R – reaction rim.

texture essentially composed of interlocking inequigranular crystals mainly of calcite of variable size with minor apatite, into a granular fabric (Figure 4d). The crystalline calcite portions also contain poikilitic intergrowths of phlogopite as an important accessory mineral (black in plain polarised light) and haematite (dark brown) (Figure 4e). Although the contact of crystalline calcite and kimberlite is sharply defined, at places, it shows an intermixing nature (Figure 4f). As a whole, the calcite occurs as clear granular aggregate and also as needle-like shapes. The latter resembles quenched magmatic calcite from some kimberlite sills similar to South African pipes. Hence, a possible carbonatite genesis is also envisaged as the overall texture and mineralogy of calcite phase suggesting a magmatic nature because of the way it penetrates spaces between former adjacent macrocrystals. Thus it is presumed to be a carbonatite (sovite) phase. Thus, the 5119 pipe rock is classified as clast supported hypabyssal macrocrystic kimberlite breccia associated with carbonatite (?) phase.

Geochemistry

Major, trace and rare earth element data (see Table 3 in [*Phani et al.,* 2020]) has been used to plot various binary and ternary diagrams to decipher the geochemical character of the two Gooty pipes under investigation. The data of the two kimberlites has been compared with that of average Wajrakarur pipes [*Chalapathi Rao et al.,* 2004], Chelima lamproite [*Chalapathi Rao et al.,* 2007], Khaderpet pipe with carbonatite [*Smith et al.,* 2013] and southern African Group-I kimberlite pipes [*Le Roex et al.,* 2003].

The major and trace element data of the two kimberlites under present study clearly indicates that their chemical composition is broadly akin to that of WKF and South African pipes. The TiO_2 content in the 5023 pipe ranges from 1.51–1.61 (wt%) which is less than that of Wajrakarur kimberlites and Chelima lamproite but similar to South African Group-I pipes. Similarly, the Mg# for the 5023 pipe (79.07 to 80.84) and 5119 kimberlite rich samples (72.1 to 74.35) are in line with those of WKF and South African pipes. The exceptional cases are 5119 samples rich in carbonatite (?) possessing a lower Mg# (37.54 to 57.58) than the kimberlite rich samples (72.1 to 74.35). In addition, 5119

carbonatite (?) rich samples possess a higher amount of CaO (50.25 to 52.35 wt%) than the kimberlite-rich samples (14.56 to 18.45 wt%). The ΣREE ranging from 440.62 to 469.95 and from 496.8 to 508.22 in 5023 and 5119 kimberlite rich samples respectively, is similar to Group-I varieties. The crystalline calcite rich samples of the 5119 pipe, the ΣREE ranges from 168.66 to 174.88. The La/Yb ratios in kimberlites are significantly higher (50–200) than in the other mantle rocks and the EDC kimberlites are characterised by La/Yb ratio of 70–170 and enrichment of LREE relative to MREE with La/Sm ratios ranging from 7–20 [*Chalapathi Rao,* 2008]. This is well applicable to 5023 (147.38–178.57) and 5119 (52.41–150.07); the lowest being in the 5119 carbonatite (?) rich samples. In the 5023 pipe, the La/Sm ratio ranges from 11.07–12.32 while that in the 5119 pipe, 8.16–11.75, close to those of Group-I pipes. Furthermore, it is observed that the secondary surficial processes and crustal contamination by sedimentary rocks in these kimberlites have not disturbed the REE concentrations of the kimberlites. Thus, based on the overall geochemical characteristic, the 5023 and 5119 pipes are categorised as archetypal Group-I varieties, which is demonstrated by various geochemical diagrams.
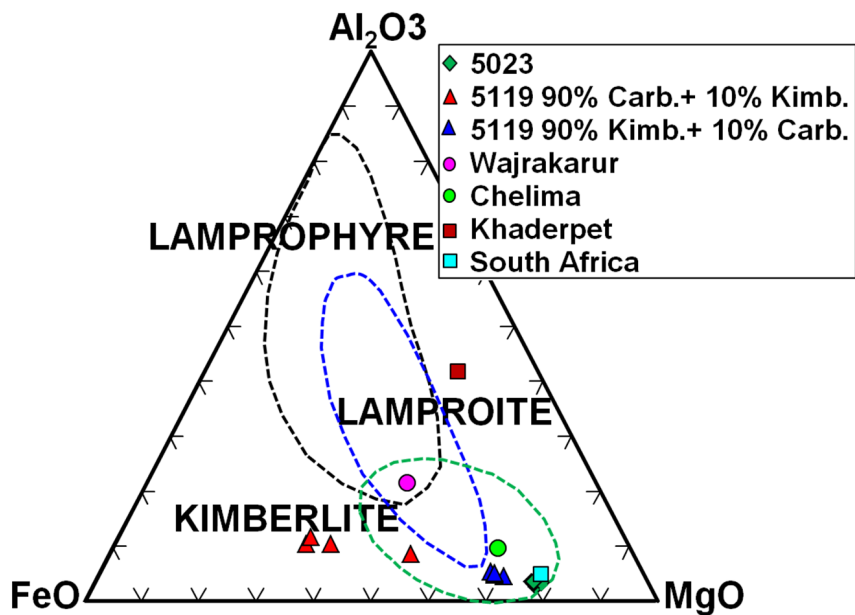
Figure 5. Ternary plot of Al_2O_3-FeO-MgO. Fields after [*Bergman,* 1987].

In the ternary diagram involving K_2O, MgO and Al_2O_3, the 5023 and 5119 samples plot in the kimberlite field along with South African and WKF kimberlites (Figure 5). In the bivariate diagram involving Fe and Si (cationic weight %) also, the 5023 and 5119 samples plot in the Group-I field (Figure 6a). The crustal contamination index (C.I.), determined using the below formula, provides inferences on the degree of contami-

nation and helps to assess the role of crustal assimilation on the bulk chemistry of the kimberlites [*Clement,* 1982]:

$$C.I. = (SiO_2 + Al_2O_3 + Na_2O)/(MgO + 2K_2O)$$

Uncontaminated kimberlites possess a C.I. of less than 1.4. The C.I. is directly proportional to the SiO_2 and Al_2O_3 concentrations in kimberlites; < 35 wt% and < 5 wt% indicate fresh kimberlites [*Mitchell,* 1986]. Except 5119 samples with 10% kimberlite, both the pipes are uncontaminated (see Table 3 in [*Phani et al.,* 2020]). The bivariate diagram between CaO (wt%) and crustal contamination index (C.I.) reveals that the 5023 and kimberlite-rich 5119 samples plot in the "non-carbonate" field while the 5119 samples with 10% kimberlite plot in the "highly carbonated" field which is consistent with field and petrographic observations (Figure 6b). Variations in trace element concentrations also clearly show that 5119 and 5023 kimberlites are of Group-I type. For instance, the Ce versus Ce/Pb ratio diagram indicates an affinity of the two pipes towards Group-I type (Figure 6c). The binary diagram between La/Nb and Th/Nb evidently shows that 5119 and 5023 samples are similar to Group-I kimberlites of

South Africa and other EDC pipes (Figure 6d). Thus geochemically, the 5119 and 5023 pipes show archetypal Group-I kimberlitic character akin to majority of EDC kimberlites. The chondrite normalized [*Sun and McDonough,* 1989] REE patterns reveal a high proportion of LREE and low content of HREE. The two Gooty pipes conspicuously show a step-like REE pattern similar to South Africa, WKF, Khaderpet kimberlites and Chelima lamproite (Figure 7). This indicates a high degree of fractionation at the time of kimberlite magma ascent [e.g. *Nadeau,* 2016]. The LREE enrichment (1000 x chondrite), absence of positive Eu anomalies and the low HREE and Y contents of the Gooty cluster samples under this study, offer additional evidence of no impact of crustal contamination on the kimberlite chemistry.

Petrogenesis

Using whole rock geochemical data, the petrogenesis of the two pipes under present study have been deciphered. The Ilmenite Index (Ilm.I.), calculated by below formula, identifies kimberlites that may have accumulated ilmenite megacrysts and xenocrysts. The kimberlites with an "Ilm. I." less than 0.52 are regarded as
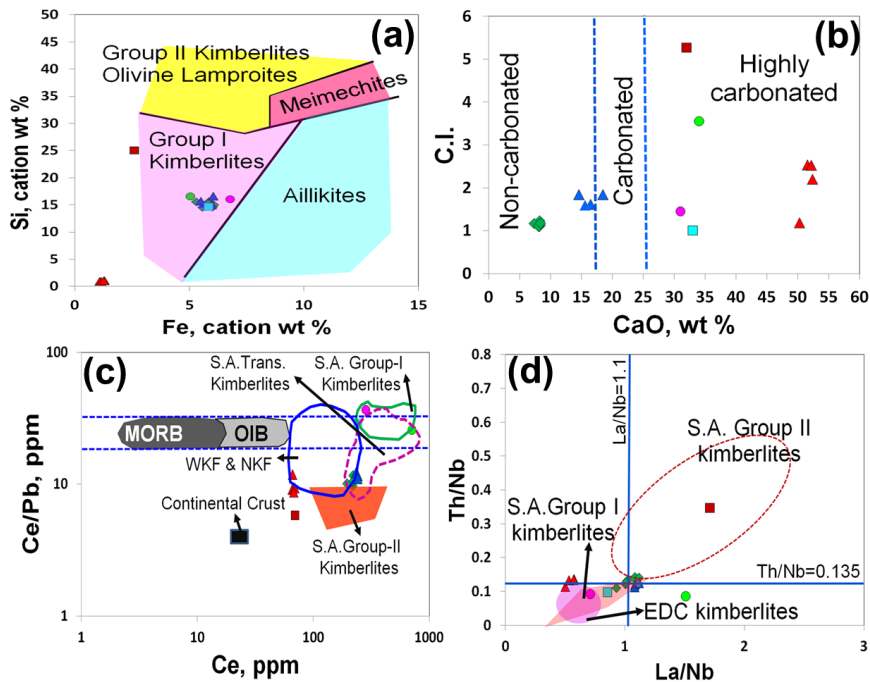
Figure 6. (a) Binary plot between cationic weight percentages of Fe and Si, showing Group-I kimberlitic character of 5023 and 5119 pipes [*Williams-Jones et al.,* 2004]. (b) CaO versus crustal contamination index (C.I.) plot showing non-carbonated nature of 5023 and non-carbonated to hi8ghly carbonated nature of 5119 kimberlite [*Taylor et al.,* 1994]. (c) Ce versus Ce/Pb diagram. Fields for South African (S.A.) Group-I and II kimberlites are from Le [*Becker and Le Roex,* 2006; *Le Roex et al.,* 2003]; WKF and NKF from *Chalapathi Rao et al.* [2004] and *Chalapathi Rao and Srivastava* [2009]. (d) La/Nb versus Th/Nb diagram. Fields for South African (S.A.) kimberlites after *Becker and Le Roex* [2006] and *Coe et al.* [2008]; fields for EDC kimberlites adopted from *Chalapathi Rao et al.* [2004]. Symbols as in Figure 5.
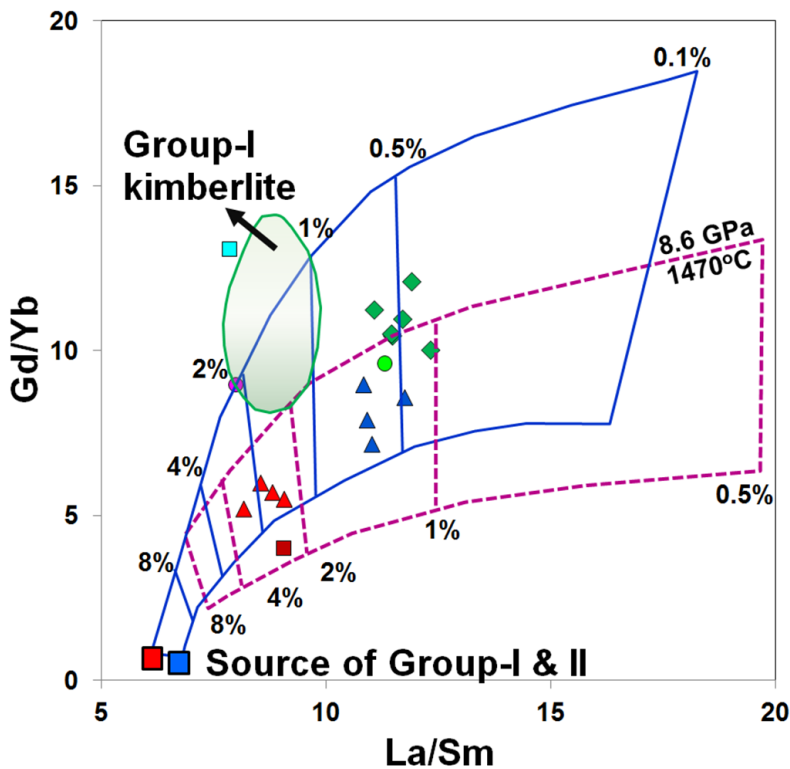
Figure 7. La/Sm versus Gd/Yb for the 5023 and 5119 kimberlites. Illustrated curves in blue representing melting trajectories of inferred source-regions for Group-I and Group-II kimberlites, field for Group-I kimberlites are from *Becker and Le Roex* [2006] while the purple dashed lines represent melting curves from experimentally determined bulk peridotite/melt partition coefficients from *Dasgupta et al.* [2009]. The Group-I and Group-II kimberlites possess the residual mineralogy: ol:opx:cpx:grt = 0.67 : 0.26 : 0.04 : 0.03; ol:opx:cpx:grt = 0.67 : 0.26 : 0.06 : 0.01 respectively. Numbers represent the degree of melting (%). Adopted from *Dongre et al.* [2016]. Symbols as in Figure 5.

uncontaminated [*Taylor et al.,* 1994].

$$Ilm.I = (FeO_T + TiO_2)/(2K_2O + MgO)$$

While the "Ilm.I." is within the limit for both the pipes, the carbonatite (?) rich 5119 samples show higher range due to carbonatite association (see Table 3 in [*Phani et al.,* 2020]). Therefore, the C.I. and Ilm.I. values have little effect on the major element composition of the GKC pipes of this study. The REE patterns considering variation between the ratios of La/Sm and Gd/Yb reveal that the Gooty pipes under present study might have originated from a very low partial melting at a range of ~ 0.5 to 2.5% according to the petrogenetic model of *Becker and Le Roex* [2006] whereas according to melting trajectories calculated based on partition coefficient values given by *Dasgupta et al.* [2009], the kimberlites plot within a range of $1-4\%$ similar to South African, WKF pipes, Khaderpet and Chelima lamproite. A higher partial melting range is observed in the 5119 samples in which carbonatite (?) proportion is high (Figure 8).

It is noticed that crystalline calcite phase, presumed to be carbonatite, occurs as a distinct massive, brecciated and intimately associated entity with 5119 kim-
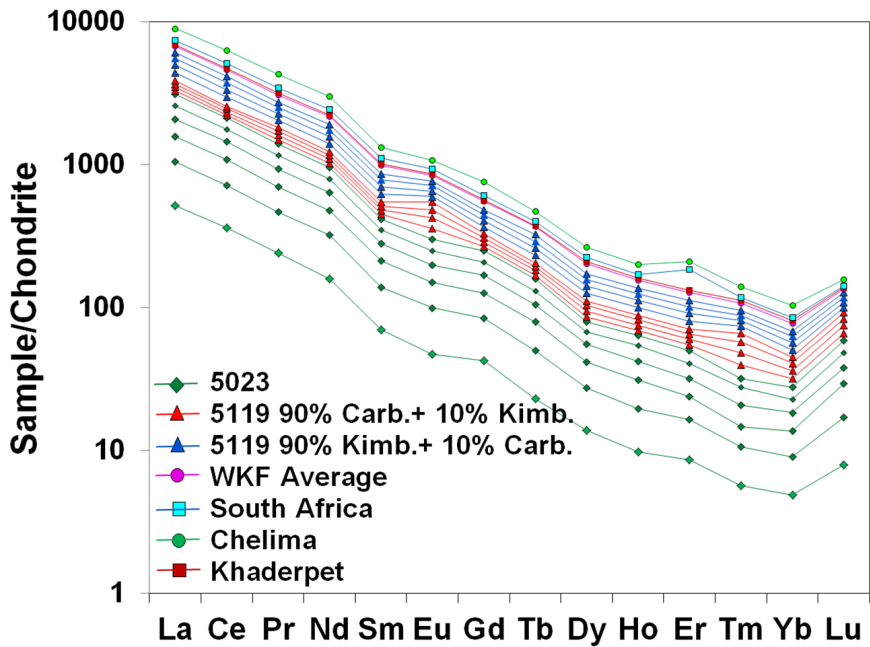
Figure 8. Chondrite normalized [*Sun and McDonough,* 1989] rare earth element concentrations in 5023 and 5119 kimberlites.

berlite favouring magmatic origin, owing to the accumulated field, petrographic and geochemical studies. The presence of primary carbonatite phase is also supported by the enrichment of trace elements like Nb (78.3 to 87 ppm), Ba (6745 to 8685 ppm), Sr (203–234 ppm) etc. in 5119 samples [*Mitchell,* 2005]. A slight positive correlation between La/Sm and Nb in

5023 and 5119 kimberlites indicates involvement of carbonated melt or source [*Prelević et al.,* 2008]. The genetic relation between kimberlite clan rocks and carbonatites has been a subject of great debate [e.g. *Mitchell,* 1979; *Tappe et al.,* 2008, 2013]. Although the genetic link between archetypal kimberlites and carbonatites sensu stricto may be controversial [*Smith et al.,* 1985], the case for closely related rock types is attaining significance as evidenced in the ultramafic lamprophyres (aillikites) and carbonatites in Greenland [*Tappe et al.,* 2006, 2009 2011], Labrador, Quebec [*Tappe et al.,* 2008] and Manitoba [*Chakhmouradian et al.,* 2009]. In the Indian context, the association of carbonatites and kimberlite clan rocks has been reported at Khaderpet, Andhra Pradesh (ultramafic lamprophyre) and Sidhi, Madhya Pradesh (lamproite) [*Chatterjee et al.,* 2008; *Smith et al.,* 2013; *Satyanarayanan et al.,* 2017].

The field and petrographic studies on kimberlites of present study revealed suspected presence of carbonatite with the 5119 pipe. Stable isotopes of carbon and oxygen have been proved to be useful in distinguishing primary igneous carbonatites and marine carbonates. The stable isotope analysis of crystalline calcite in 5119 has markedly indicated the pristine character-

istics of primary igneous or magmatic carbonatite. In the primary carbonatites, variations in stable isotopes of C and O (δ^{13}C and δ^{18}O) occur essentially due to fractional crystallization. The δ^{13}C values range from -9 to $-1‰$ whereas δ^{18}O values range from $+5$ to $+15‰$ [*Plyusnin et al.,* 1980; *Deines,* 1989]. The δ^{13}C and δ^{18}O variations of crystalline calcite of 5119 kimberlite samples plot within the field defined for primary carbonatites (Figure 9). Thus, the accumulated petrographic, geochemical and stable isotopic evidences indicate that the 5119 pipe is associated with carbonatite phase, which could be sovite variety. Thus, association of carbonatite with 5119 kimberlite is not an uncommon feature and it is expected to be of critical value in elucidating the kimberlite-carbonatite metallogeny and tectonomagmatic evolution of this part of the craton.

Whole rock geochemical evidences as shown in the binary diagram between Fe_2O_3 (wt%) and Y (ppm) wherein the samples of 5023 and 5119 kimberlites characteristically plot in the "prospective kimberlite" field while the carbonatite rich samples of 5119 plot outside the field due to the presence of less amount of kimberlite material in the samples (Figure 10). This is consistent with field exploration reports of the CRAEI that both these kimberlites are diamondiferous. How-
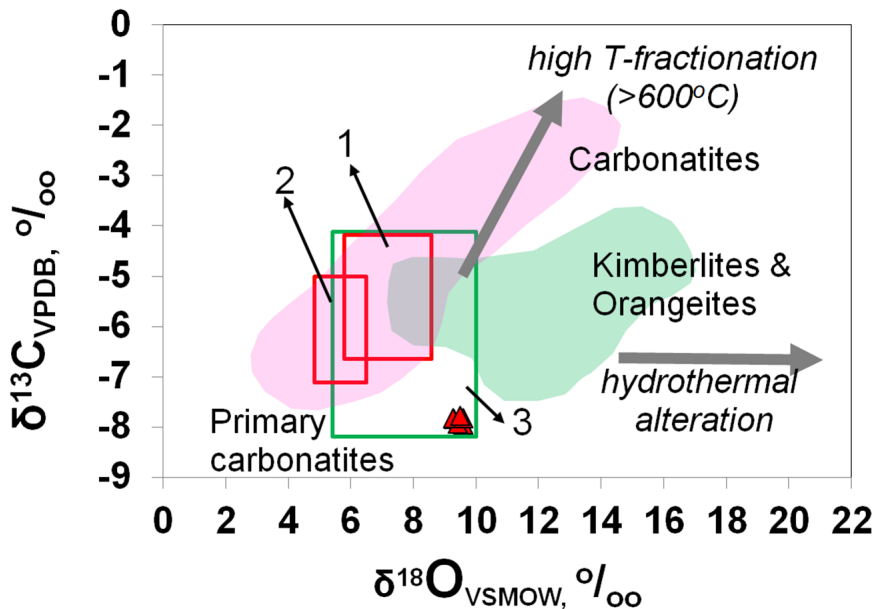
Figure 9. Carbon and Oxygen stable isotope compositions (in ‰ relative to V-PDB and V-SMOW respectively), showing primary carbonatite nature of crystalline calcite rich 5119 samples. Fields for (a) primary carbonatite fields: 1 – *Clarke et al.* [1994]; 2 – *Keller and Hoefs* [1995] and 3 – *Taylor et al.* [1967] and (b) fields for carbonatites, kimberlites and orangeites after *Tappe et al.* [2006]. Symbols as in Figure 5.

ever, both the pipes deserve detailed investigations to ascertain their economic diamond potentiality. As a whole, the analyses of this investigation reveal that the 5023 and 5119 intrusions are archetypal Group-I kimberlites, with the latter associated possible carbon-
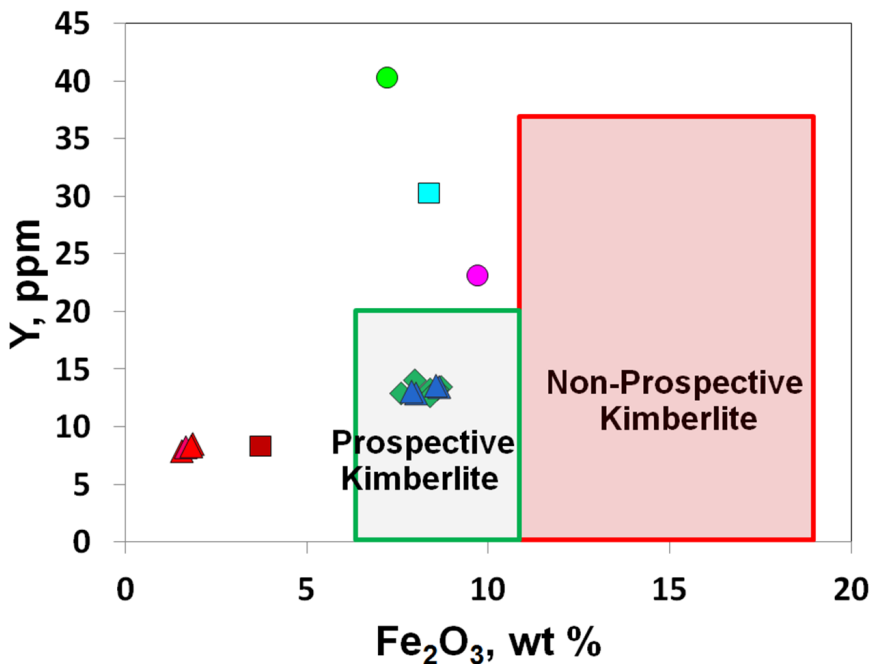
Figure 10. Binary diagram between Fe_2O_3 and Y showing diamondiferous nature of 5023 and 5119 kimberlites. [*Birkett,* 2008]. Symbols as in Figure 5.

atite, that warrant detailed studies on their time of emplacement, to have an enhanced understanding of geodynamic evolution of the craton and the sedimentary basin.

Conclusion

The diamondiferous kimberlites of present study (5023 and 5119) are emplaced into carbonate and siliciclastic sediments such as dolomite, dolomitic limestone, shale etc. of Vempalli Formations, on the western flank of Cuddapah basin of Palaeoproterozoic age. Both the kimberlites are classified as macrocrystic hypabyssal kimberlite breccias of archetypal Group-I variety on the basis of petrographic and whole rock geochemical evidences. The 5119 kimberlite appears to be unique in possessing carbonatite (sovite) phase which is well supported by field, petrographic, geochemical and stable isotope analyses of this study. Both the kimberlites appear to have originated from low degree of partial melting (0.5–2%), emplaced along a deep-seated fault. Owing to the presence of xenoliths of dolomite, shale, cherty dolomite etc. identical with Vempalli Formation forming the country, it is clear that these pipes have erupted post-lower Cuddapah Formations. The possible association of carbonatite (?) phase with the 5119 kimberlite certainly warrants further detailed mineralogical, petrological and geochronological investigations. Nevertheless, these discoveries unravel a new panorama for diamond explorationists to discover many

such kimberlites and related rock types within the vast Proterozoic Cuddapah synclinorium.

References

Becker, M., A. P. Le Roex (2006) , Geochemistry of South African on and off-craton Group I and II kimberlites: petrogenesis and source region evaluation, *Journal of Petrology*, *47*, p. 67–703, **Crossref**

Bergman, S. C. (1987) , Lamproites and other Potassium rich alkaline rocks; a review of their occurrence, mineralogy and geochemistry, *Alkaline Igneous Rocks. Fitton J. G. and Upton B. J. (Eds.), Special Publication No. 30*, p. 103–190, Geological Society of London, UK, **Crossref**

Birkett, T. C. (2008) , First-row transition elements, Y and Ga in kimberlite and lamproite: applications to diamond prospectivity and petrogenesis, *Canadian Mineralogist*, *46*, p. 1269–1282, **Crossref**

Chakhmouradian, A. R., C. O. Bohm, A. Demeny, et al. (2009) , "Kimberlite" from Wekusko Lake, Manitoba: actually a diamond-indicator-bearing dolomite carbonatite, *Lithos*, *112S*, p. 347–357, **Crossref**

Chalapathi Rao, N. V. (2007) , Chelima Dykes, Cuddapah Basin, Southern India: A Review of the Age, Petrology, Geochemistry and Petrogenesis of World's Oldest Lamproites, *Journal of Geological Society of India*, *69*, p. 523–538.

Chalapathi Rao, N. V. (2008) , Precambrian Alkaline Potassic-Ultrapotassic, Mafic-Ultramafic Magmatism in Peninsular India, *Journal of Geological Society of India*, *72*, p. 57–84.

Chalapathi Rao, N. V. (2012) , Book Reviews "Diamonds and their Source Rocks in India", Authored by Fareeduddin and R. H.

Mitchell. Geological Society of India, 434 p., *Current Science*, *103*, no. 9, p. 1107–1109.

Chalapathi Rao, N. V., R. K. Srivastava (2009) , Petrology and geochemistry of diamondiferous Mesoproterozoic kimberlites from Wajrakarur kimberlite field, eastern Dharwar craton, southern India: genesis and constraints on mantle source regions, *Contributions to Mineralogy and Petrology*, *157*, p. 245–265, **Crossref**

Chalapathi Rao, N. V., S. A. Gibson, et al. (2004) , Petrogenesis of Proterozoic lamproites and kimberlites from the Cuddapah Basin and Dharwar craton, southern India, *Journal of Petrology*, *45*, no. 5, p. 907–948, **Crossref**

Chalapathi Rao, N. V., A. N. Dongre, et al. (2016) , A Late Cretaceous (ca. 90 Ma) kimberlite event in southern India: Implication for sub-continental lithospheric mantle evolution and diamond exploration, *Gondwana Research*, **Crossref**

Chatterjee, B., S. E. Haggerty, et al. (2008) , Kimberlite-carbonatite relationships revisited: evidence from Khaderpet pipe, Andhra Pradesh, India, *9th International Kimberlite Conference Extended Abstract No. 9IKC-A-00070*, p. 1–3, University of Alberta, Canada.

Clarke, L. B., M. J. Le Bas, B. Spiro (1994) , Rare earth, trace element and stable isotope fractionation of carbonatites at Kruidfontein, Transvaal, South Africa, *Meyer, H. O. A. and Leonardos, O. H. (eds.), Kimberlites, Related Rocks and Mantle Xenoliths*, p. 236–251, Companhia de Pesquisa de Recursos Minerais, Rio de Janeiro.

Clement, C. R. (1982) , , Ph. D. Thesis, Rodenbosch, South

Africa, University of Cape Town.

Coe, N., A. P. Le Roex, J. J. Gurney, et al. (2008) , Petrogenesis of Swartruggens and Star Group II kimberlite dyke swarms, South Africa: constraints from whole rock geochemistry, *Contributions to Mineralogy and Petrology*, *156*, p. 627–652, **Crossref**

CRAEI, (2004) , , GOMS No. 24–27 Vol. 1 0f 5, from Jan. 2001 to Feb. 2004, CRA Exploration (India) Pvt. Limited (RioTinto Group), India (http://www.ibm.nic.in/).

Das Sharma, S., D. S. Ramesh (2013) , Imaging mantle lithosphere for diamond prospecting in southeast India, *Lithosphere*, *5*, no. 4, p. 31–342, **Crossref**

Dasgupta, R., M. M. Hirschman, et al. (2009) , Trace element partitioning between garnet lherzolite and carbonatite at 6.6 and 8.6 GPa with applications to the geochemistry of the mantle and of mantle derived melts, *Chemical Geology*, *262*, p. 57–77, **Crossref**

Dawson, J. B. (1980) , *Kimberlites and Their Xenoliths*, Springer Verlag, Heidelberg Press, N.Y, **Crossref**

Dawson, J. B., M. S. Garson, B. Roberts (1987) , Altered former alkali carbonatite lava from Oldoinyo Lengai, Tanzania: Inferences for calcite carbonatite lavas, *Geology*, *15*, no. 8, p. 765–768, **Crossref**

Deines, P. (1989) , Stable isotope variations in carbonatites, *Carbonatites: Genesis and Evolution, Bell, K. (ed.)*, p. 301–359, Unwin Hyman, London.

Dongre, A. N., N. V. Chalapathi Rao, et al. (2016) , Petrology, genesis and geodynamic implication of the Mesoproterozoic– Late Cretaceous Timmasamudram kimberlite cluster, Wajrakarur

field, Eastern Dharwar Craton, southern India, *Geoscience Frontiers*, *8*, no. 3, p. 541–553, **Crossref**

Kale, V. S. (2016) , Proterozoic Basins of Peninsular India: Status within the Global Proterozoic Systems, *Proceedings of the Indian National Science Academy*, *82*, no. 3, p. 461–477, **Crossref**

Keller, J., J. Hoefs (1995) , Stable isotope characteristics of recent natrocarbonatite from Oldoinyo Lengai, *Carbonatite Volcanism: Oldoinyo Lengai and the Petrogenesis of Natrocarbonatites, Bell, K. and Keller, J. (eds.)*, p. 113–123, Springer, Berlin, **Crossref**

Le Roex, A. P., D. R. Bell, P. Davis (2003) , Petrogenesis of Group I kimberlites from Kimberley, South Africa: evidence from bulk rock geochemistry, *Journal of Petrology*, *44*, p. 2261–2286, **Crossref**

Mitchell, R. H. (1979) , The alleged kimberlite–carbonatite relationship: additional contrary mineralogical evidence, *American Journal of Science*, *279*, p. 570–589, **Crossref**

Mitchell, R. H. (1986) , *Kimberlites: Mineralogy, Geochemistry and Petrology*, 442 pp., Plenum Press, New York and London.

Mitchell, R. H. (2005) , Carbonatites and carbonatites and carbonatites, *Canadian Mineralogist*, *43*, p. 2049–2068, **Crossref**

Nadeau, O., R. Stevenson, M. Jebrak (2016) , Evolution of Montviel alkaline-carbonatite complex by coupled fractional crystallisation, fluid mixing and metasomatism, Part II: Trace element and Sm–Nd isotope geochemistry of metasomatic rocks; Implications for REE Nb mineralisation, *Ore Geology Reviews*, *72*, p.

1163–1173, **Crossref**

Nagaraja Rao, B. K., S. T. Rajurkar, et al. (1987) , Stratigraphy, structure and evolution of the Cuddapah Basin, *Geological Society of India Memoir*, *6*, p. 33–86.

Phani, P. R. C. (2015) , Area selection for Diamond Exploration based on Geological and Morphostructural setup: Examples from Wajarakarur Kimberlite Field, India, *Journal of Advanced Chemical Sciences*, *1*, p. 102–106.

Phani, P. R. C., V. V. N. Raju (2017) , A New Kimberlite pipe in Balkamthota Vanka, Pennahobilam, Anantapur district, Andhra Pradesh, India. Field aspects and Preliminary investigations, *Periodico di Mineralogia*, *86*, no. 3, p. 213–228, **Crossref**

Phani, P. R. C., P. Sengupta, S. Basu (2020) , Data on geochemistry and petrology of two kimberlites at Krishtipadu, Andhra Pradesh, Southern India, Earth Science DataBase, GC RAS, Moscow, **Crossref**

Plyusnin, G. S., V. S. Samoylov, S. I. Gol'shev (1980) , The δ^{13}C, δ^{18}O isotope pair method and temperature facies of carbonatites, *Doklady Akademi Nank USSR. Seriya Geologiya*, *254*, p. 1241–1245.

Prelevi, D., S. F. Foley, et al. (2008) , Mediterranean tertiary lamproites derived from multiple source components in post collisional geodynamics, *Geochimica et Cosmochimica Acta*, *72*, p. 2125–2156, **Crossref**

Radhakrishna, B. P. (2007) , Diamond exploration in India: Retrospect and prospect, *Journal of Geological Society of India*, *69*, p. 419–442.

Ravi, S., K. S. Bhaskara Rao, R. Ananda Reddy (2018) , Diamond

Fields of India, *Bulletin Series A, Geological Survey of India*, *68*, p. 1033.

Saha, D., V. Tripathy (2012) , Palaeoproterozoic sedimentation in the Cuddapah Basin, south India and regional tectonics: A review, *Palaeoproterozoic of India, Mazumdar, R. and Saha, D. (eds.), Special Publication, 365*, p. 161–184, Geological Society of India, India, **Crossref**

Satyanarayanan, M., D. V. S. Rao, et al. (2017) , Petrogenesis of carbonatitic lamproitic dykes from Sidhi gneissic complex, Central India, *Geoscience Frontiers*, p. 1–27, **Crossref**

Shaikh, A. M., S. C. Patel, et al. (2016) , Mineralogy of the TK1 and TK4 "kimberlites" in the Timmasamudram cluster, Wajrakarur Kimberlite Field, India: Implications for lamproite magmatism in a field of kimberlites and ultramafic lamprophyres, *Chemical Geology*, **Crossref**

Smith, C. B., H. L. Allsopp, et al. (1985) , Emplacement ages of Jurassic-Cretaceous South African kimberlites by the Rb–Sr method on phlogopite and whole-rock samples, *Transactions of Geological Society of South Africa*, *88*, p. 249–266.

Smith, C. B., S. E. Haggerty, et al. (2013) , Kimberlite, lamproite, ultramafic lamprophyre, and carbonatite relationships on the Dharwar Craton, India; an example from the Khaderpet pipe, a diamondiferous ultramafic with associated carbonatite intrusion, *Lithos*, *182–183*, p. 102–113, **Crossref**

Sun, S.-s., W. F. McDonough (1989) , Chemical and Isotopic systematics of oceanic basalts: implications for mantle compositions and processes, *Magmatism in the Oceanic Basins, Saunders A. D. and Norry M. J. (eds.), Special Publication, 42*, p.

313–345, Geological Society, India, **Crossref**

Tappe, S., S. F. Foley, G. A. Jenner, et al. (2006) , Genesis of ultramafic lamprophyres and carbonatites at Ailik Bay, Labrador, a Cosequence of Incipient Lithospheric Thinning beneath the North Atlantic Craton, *Journal of Petrology*, *476*, no. 7, p. 1261–1315, **Crossref**

Tappe, S., S. F. Foley, et al. (2008) , Between carbonatite and lamproite- diamondiferous Torngat ultramafic lamprophyres formed by carbonate-fluxed melting of cratonic MARID-type metasomes, *Geochemica et Cosmochimica Acta*, *72*, p. 3258–3286, **Crossref**

Tappe, S., A. Steenfelt, et al. (2009) , The newly discovered Jurassic Tikiusaaq carbonatite–aillikite occurrence, West Greenland, and some remarks on carbonatite–kimberlite relationships, *Lithos*, *112S*, p. 385–399, **Crossref**

Tappe, S., G. D. Pearson, G. Nowell, et al. (2011) , A fresh look at Greenland kimberlites: cratonic mantle lithosphere imprint on deep source signal, *Earth and Planetary Science Letters*, *305*, p. 235–248, **Crossref**

Tappe, S., G. D. Pearson, D. Prelevic (2013) , Kimberlite, carbonatite, and potassic magmatism as part of the geochemical cycle, *Chemical Geology*, **Crossref**

Taylor, H. P., J. Frechen, E. T. Degens (1967) , Oxygen and carbon isotope studies of carbonatites from the Laacher See District, West Germany and the Alnö District, Sweden, *Geochimica et Cosmochimica Acta*, *31*, p. 407–430, **Crossref**

Taylor, W. R., L. A. Tomkins, S. E. Haggerty (1994) , Comparitive geochemistry of West African kimberlites: Evidence for a mi-

caceous kimberlite end member of sub-lithospheric origin, *Geochemica et. Cosmochemica Acta*, *58*, p. 4017–4037, **Crossref**

Williams-Jones, A. E., J. Hartzler, et al. (2004) , *A geochemical approach to the classification of kimberlitic rocks Divex Rapport Final, Sous-project SC8a*, 8 pp., MgGill University, Montréal.